Article

Biophysical Studies of Bacterial Topoisomerases Substantiate Their Binding Modes to an Inhibitor

CongBao Kang,[1,*] Yan Li,[1] Joseph Cherian,[1] Boping Liu,[1] Hui Qi Ng,[1] Michelle Yueqi Lee,[1] Nur Huda Binte Ahmad,[1] Zhi Ying Poh,[1] Yun Xuan Wong,[1] Qiwei Huang,[1] Ying Lei Wong,[1] Alvin W. Hung,[1] Jeffrey Hill,[1] and Thomas H. Keller[1,*]

[1]Experimental Therapeutics Centre, Agency for Science, Technology and Research (A*STAR), Singapore

ABSTRACT Bacterial DNA topoisomerases are essential for bacterial growth and are attractive, important targets for developing antibacterial drugs. Consequently, different potent inhibitors that target bacterial topoisomerases have been developed. However, the development of potent broad-spectrum inhibitors against both Gram-positive (G^+) and Gram-negative (G^-) bacteria has proven challenging. In this study, we carried out biophysical studies to better understand the molecular interactions between a potent *bis*-pyridylurea inhibitor and the active domains of the E-subunits of topoisomerase IV (ParE) from a G^+ strain (*Streptococcus pneumoniae* (sParE)) and a G^- strain (*Pseudomonas aeruginosa* (pParE)). NMR results demonstrated that the inhibitor forms a tight complex with ParEs and the resulting complexes adopt structural conformations similar to those observed for free ParEs in solution. Further chemical-shift perturbation experiments and NOE analyses indicated that there are four regions in ParE that are important for inhibitor binding, namely, α2, the loop between β2 and α3, and the β2 and β6 strands. Surface plasmon resonance showed that this inhibitor binds to sParE with a higher K_D than pParE. Point mutations in α2 of ParE, such as A52S (sParE), affected its binding affinity with the inhibitor. Taken together, these results provide a better understanding of the development of broad-spectrum antibacterial agents.

INTRODUCTION

The discovery of novel antibacterial agents is of great interest because drug-resistant bacteria have become a serious problem (1–3). In recent years, new antibiotics such as tigecycline and carbapenems (1,4) have been approved to tackle drug-resistant bacteria. However, resistance against these newly developed compounds usually emerges rapidly after they have been introduced into clinical practice (5–7). Therefore, there exists a great need for new antibacterial agents, especially compounds with a novel mechanism of action (8,9).

The bacterial DNA topoisomerases are attractive drug targets because of their importance in DNA replication and their low homology with eukaryotic topoisomerases (8–10). Bacterial DNA topoisomerases are essential for bacterial growth because they control the interconversion of different topological forms of DNA. Unlike eukaryotic topoisomerases, prokaryotic topoisomerases are functional as heterotetramers. Bacteria express two forms of type II topoisomerases: DNA gyrase and topoisomerase IV (Topo IV) (8). DNA gyrase can relax supercoiled plasmid DNA and plays an important role in DNA replication and transcription (11). Topo IV is required for proper chromosome separation and plays an important role in the maintenance of DNA supercoiling in bacteria. Both of these topoisomerase II molecules exist as protein complexes made up of two subunits: GyrA and GyrB for gyrase, and ParC and ParE for Topo IV. Both GyrB and ParE have similar structures and have been pursued as drug targets by a number of groups (12–14).

The prototypical inhibitor of GyrB and ParE is the natural product novobiocin, an aminocoumarin that binds to the ATP site (15–17). Structure-based design has been used for the optimization of a number of scaffolds, and potent inhibitors that target both GyrB and ParE have been identified (12,13,18). We were interested in using a structure-based approach to design GyrB/ParE inhibitors for Gram-negative (G^-) bacteria, especially *Pseudomonas aeruginosa* (*P. ae*). Previous approaches for structure-based optimization have often relied on available GyrB/ParE x-ray structures from *Escherichia coli* and *Streptococcus pneumonia* (*S. pn*) (12,13,18–21). However, it is unclear whether these structures are suitable for the design of inhibitors that target ESKAPE pathogens (*Enterococcus faecium*, *Staphylococcus aureus*, *Klebsiella pneumonia*, *Acinetobacter baumannii*, *P. ae*, and *Enterobacter species*) (12).

In this report, we describe the results of our structural analysis of ParE in solution using NMR spectroscopy. The binding of an inhibitor against ParE was characterized by surface plasmon resonance (SPR). In this study, we used two ParEs containing the 24 kDa fragment of the E-subunit of Topo IV: sParE from a Gram-positive (G^+) strain (*S. pn*) and pParE from a G^- strain (*P. ae*). First, using NMR, we showed that both ParEs bind to a pyridylurea inhibitor. Second, we obtained backbone resonance assignments for these

Submitted July 16, 2015, and accepted for publication October 1, 2015.

*Correspondence: cbkang@etc.a-star.edu.sg or thkeller@etc.a-star.edu.sg

Editor: Jeff Peng.

0006-3495/15/11/1969/9

http://dx.doi.org/10.1016/j.bpj.2015.10.001

two ParEs in the absence and presence of the inhibitor to understand the solution structures of the ParEs. Third, we conducted chemical-shift perturbation (CSP) experiments to compare inhibitor binding. Fourth, we analyzed the ParE-inhibitor complexes using nuclear Overhauser enhancements (NOEs) between the protein and the inhibitor. Lastly, using SPR, we tested the binding affinity between the inhibitor and ParEs and their mutants in the $\alpha 2$ helix. Our results suggest that the inhibitor binds to both pParE and sParE in the same mode. However, minor changes in the amino acid in the protein sequence gave rise to a significant discrepancy in the magnitude of inhibitor binding.

MATERIALS AND METHODS

Sample preparation

To produce ParEs, cDNA encoding sParE encompassing residues 1–228 of the E-subunit of Topo IV of *S. pn* was synthesized by Genscript. cDNA encoding pParE encompassing residues 1–218 of the E-subunit of Topo IV of *P. ae* was amplified using the genome of *P. ae* as a template. The cDNA of sParE or pParE was cloned into the NdeI and XhoI sites of the pET29b, respectively. The resulting plasmid encodes the N-terminal active domain of ParE, with an extra tag containing seven residues (EHHHHHH) at the C-terminus for protein purification. To express ParEs from *E. coli* for NMR studies, the plasmid was transformed in *E. coli* (BL21DE3)-competent cells and plated onto an LB plate containing antibiotics. The protein was expressed and purified using a protocol similar to that described by Kim et al. (22). Briefly, several colonies from the LB plate were picked up and inoculated in 20 mL of M9 medium. The overnight culture at 37°C was transferred into 1 L of M9 medium supplemented with 30 μg/mL of kanamycin. When A_{600} reached 0.6–0.8, protein was induced for 18 h at 18°C by adding β-D-1-thiogalactopyranoside to 1 mM. The *E. coli* cells were harvested by centrifugation at 8000 ×g for 10 min at 4°C. The cell pellet was resuspended in a buffer containing 20 mM sodium phosphate (pH 7.8), 500 mM NaCl, and 2 mM β-mercaptoethanol. Cells were then broken up by sonication and cell lysates were cleared by centrifugation at 20,000 × *g* and 4°C for 20 min. The protein was then purified using a gravity column with nitrilotriacetic acid saturated with nickel (Ni^{2+}-NTA) resin. Purified protein from the Ni-NTA^{2+} resin was further purified by gel filtration chromatography using a Superdex 200 column. For the sParE, protein was prepared in a buffer containing 20 mM sodium phosphate (pH 6.5), 80 mM KCl, 2 mM dithiothreitol, and 0.5 mM EDTA. For the pParE, protein was prepared in a buffer containing 20 mM sodium phosphate (pH 6.5), 180 mM KCl, 2 mM dithiothreitol, and 0.5 mM EDTA to prevent sample precipitation. To prepare a ^{13}C-, ^{15}N-, and ^{2}H-labeled protein, protein was expressed in M9 medium containing 1 g/L $^{15}NH_4Cl$, 2 g/L ^{2}H-^{13}C-glucose, and D_2O (99.9%). The protein was concentrated to 0.5–0.8 mM for NMR studies.

Backbone resonance assignment

Uniformly ^{15}N- or ^{13}C, ^{15}N-, and ^{2}H-labeled proteins were used in NMR data acquisition. For free sParE and pParE, backbone resonance was assigned based on two-dimensional and three-dimensional (3D) experiments and transverse relaxation-optimized spectroscopy (TROSY) (23,24)-based experiments, including HSQC, HNCACB, HNCOCACB, HNCA, HNCOCA, HNCACO, and HNCO. For ParEs and inhibitor complexes, the protein was mixed with the inhibitor in a molar ratio of 1:1.2. The compound was prepared in deuterated-dimethyl sulfoxide (d-DMSO) to a 60 mM concentration. The backbone resonance assignment of the sParE-inhibitor complex was referenced to the assignment of free sParE and an HNCACB experiment. For the backbone assignment of the pParE-inhibitor complex, we conducted various experiments, including ^{1}H-^{15}N-HSQC, HNCACB, HNCOCACB, HNCA, HNCOCA, HNCACO, and HNCO. All of these experiments were conducted at 25°C on a Bruker Avance 700 spectrometer. All of the pulse programs were obtained from the Topspin (2.1) pulse library. Spectra were processed with NMRPipe (25) or Topspin and analyzed using NMRView (26) and CARA (http://www.mol.biol.ethz.ch/groups/wuthrich_group). Secondary structure was predicted using TALOS+ based on the backbone chemical shifts (27).

Protein-inhibitor 1 interactions

To probe ParE and inhibitor interactions, inhibitor from a stock solution (60 mM) in d-DMSO was added into a ^{13}C-, ^{15}N-, and ^{2}H-labeled ParE sample. ^{1}H-^{15}N-HSQC spectra were acquired and processed. CSPs after the addition of inhibitor were monitored (28). The combined chemical-shift change ($\Delta\delta$) was calculated using the equation $\Delta\delta = [(\Delta\delta_{HN})^2 + (\Delta\delta_N/5)^2]^{0.5}$, where $\Delta\delta_{HN}$ is the chemical-shift changes for the amide proton dimension and $\Delta\delta_N$ is the chemical-shift changes for the amide dimension (28). To obtain protein-inhibitor intermolecular NOEs, a NOESY-TROSY experiment with a mixing time of 100 ms was recorded for a sample containing ^{13}C-, ^{15}N-, and ^{2}H-labeled ParE and inhibitor with a molar ratio of 1:1.2.

SPR measurements

SPR experiments were performed on a BIAcore-2000 system (GE Healthcare). Interactions between the ParEs and the compound were analyzed on CM5 chips. The protein was first immobilized on a CM5 sensor chip (GE Healthcare) via amine coupling. For immobilization, the system was initially primed with HEPES-buffered saline with a flow rate of 10 μL/min. The carboxylated dextran matrix was activated by a 7-min injection of a solution containing 200 mM 1-ethyl-3-(3-diethylaminopropyl)-carbodiimide and 50 mM *N*-hydroxysuccinimide. The protein was diluted to a final concentration of 20 μg/mL in 10 mM sodium acetate, pH 5, and then injected until a final immobilization level of ~5500 response units was reached. Finally, the rest of the surface was deactivated with a 7-min injection of 1 M ethanolamine hydrochloride. Binding experiments were performed at 25°C in a running buffer containing 10 mM HEPES (pH 7.5), 150 mM NaCl, 3 mM EDTA, and 0.005% v/v surfactant P20. The buffer was filtered and degassed before it was used. The compound was diluted with a running buffer before injection at a flow rate of 30 μL/min. For the binding experiment with sParE, single-cycle kinetics was used. Association was observed for 60 s and dissociation was observed for 420 s. For the binding experiment with pParE and mutants, multicycle kinetics was used. Association was observed for 60 s and dissociation was observed for 60 s. As the dissociation of the compounds from pParE was rapid, no regeneration protocol was applied. For all binding experiments, solvent correction was conducted to diminish the difference in a refractive index between the samples and running buffer. The binding data were analyzed using BIAcore T2000 Evaluation software version 2.0 (GE Healthcare). Dissociation constant (K_D) values were determined by fitting the data to a 1:1 steady-state binding model.

Structural modeling of pParE

A tertiary structural model of pParE was built using the SWISS-MODEL (29) server (http://swissmodel.expasy.org/). The x-ray crystal structure of eParE in complex with adenylyl-imidodiphosphate (Protein Data Bank (PDB) ID: 1S16) was used as a template because these two proteins have 77% sequence identity (30).

Thermal stability assay

We analyzed the thermal stability of the wild-type and mutant ParEs by using a ThermoFluor assay as described previously (31). Assay mixtures

containing 1.8 μM protein, 15× Sypro Orange dye in a buffer that contained 50 mM HEPES (pH 7.4), 250 mM NaCl, 5 mM $MgCl_2$, and 2.5% DMSO were subjected to an increase in temperature from 30°C to 80°C in 0.5°C increments at 20 s intervals. The melting temperature (T_m) was obtained from the curve.

RESULTS

Sample preparation of ParEs and an inhibitor for NMR studies

Potent ParE inhibitors have been developed by means of structure-based drug design (12–14). A class of inhibitors with pyridylurea scaffolds was shown to target the ATPase domains of topoisomerases (18). Although structures of the ATPase domains of ParE and GyrB from several bacteria have been solved using crystallography, the structures of ParE/GyrB of *P. ae*, an important pathogen, are still not available. We carried out NMR experiments to understand the differences in interactions between the ParEs of *P. ae* and *S. pn* with a *bis*-pyridylurea inhibitor. We chose to use the *bis*-pyridylurea scaffold because it was shown in a previous study (18) to have different biochemical and cell activities against ParEs from G^+ and G^- bacteria. In that study, inhibitor 1 (Fig. S1 in the Supporting Material) had a minimal inhibitory concentration (MIC) value of 2 μg/mL against *S. pn* and >64 μg/mL against *E. coli* (18). The structure of sParE with inhibitor 1 was also reported in that study and was used as a reference for our NMR studies. We expressed and purified the ATPase domains of the ParEs of both *P. ae* and *S. pn* from *E. coli* (Fig. S1). We found that pParE was not as stable as sParE, with the former showing precipitation when the protein sample was kept at room temperature for 1 day. More salt (180 mM KCl) was added to the sample buffer to prevent pParE aggregation. We synthesized a *bis*-pyridylurea inhibitor with an IC_{50} of <0.01 μM against ParE of *S. pn* as described in the literature (18).

The ParE-inhibitor 1 interaction undergoes a slow exchange

To confirm the interaction between ParEs and inhibitor 1 in solution, we carried out titration experiments by adding different amounts of inhibitor 1 to a ^{15}N-labeled sample. For both ParEs, CSP was observed, confirming their interaction with the inhibitor. When the inhibitor was titrated in the sample, free signal disappeared gradually and bound signal appeared (Fig. 1). These results suggest that the interaction undergoes a slow exchange, which is not surprising for inhibitors with a nanomolar binding affinity (18,31).

Backbone assignment and structural analysis of both ParEs

We obtained backbone assignments for the two ParEs by conducting conventional 3D experiments. For sParE, we were able to obtain a >90% backbone resonance assignment in the absence of the inhibitor, and this assignment has been deposited in the Biological Magnetic Resonance Bank (BMRB) under accession number 26610 (Fig. S2). The assignment for the ^{1}H-^{15}N-HSQC spectrum of sParE in complex with the inhibitor was obtained by referencing the assignment of its free form and analyzing the 3D-HNCACB experiment of the complex. This assignment has been deposited in the BMRB under accession number 26611 (Fig. S3). For the assignment of pParE, a >90% backbone resonance assignment was obtained first for the protein in complex with the inhibitor (BMRB accession number 26609; Fig. S3). The backbone assignment of free pParE was achieved by using conventional 3D experiments and referencing to the assignment of its inhibitor-bound form (BMRB accession number 26608; Fig. S4). With the backbone resonance assignment in hand, we conducted a secondary-structure analysis for both ParEs in the presence and absence of the inhibitor using TALOS+ (27). The secondary structures of the ParEs in the absence and presence of the inhibitor are similar to those observed in the x-ray crystal structure of the sParE-inhibitor complex, except that α1 is shorter in pParE (Fig. 2 *A*).

Structural modeling of the pParE in complex with the inhibitor

The ParE N-terminal domains (active domains) in bacteria share high sequence homology. X-ray structural studies have demonstrated that these domains contain eight β-strands backed on the side by five helices (Fig. 2 *B*) (32–34). The active domain of ParE from *E. coli* shares 77% sequence identity with pParE. We built a homology model of pParE using the x-ray crystal structure of ParE of *E. coli* (eParE) as a template (Fig. 2 *B*). Although pParE shares high sequence homology with eParE, we still analyzed the NOE spectrum to confirm the existence of the β-strand structures in the pParE model (Fig. 2 *C*). TALOS+ analysis based on backbone chemical shifts suggested that eight strands are present in pParE. To confirm the existence of the β-strands, we analyzed the NOE experiment. Longer-range NOEs between amide protons were observed (Fig. 2 *C*), suggesting that the modeled structure is reliable. The difference between the solution NMR study and model is that the modeled structure contains a longer helix α1 and α2, which may arise from the fact that this N-terminal region is more flexible in solution.

Inhibitor binding sites on ParEs determined by CSPs and NOEs

As the x-ray crystal structure of the sParE- *bis*-pyridylurea inhibitor complex was available (18), we conducted NMR studies to confirm the protein-inhibitor interaction in solution. First, we compared the chemical-shift changes

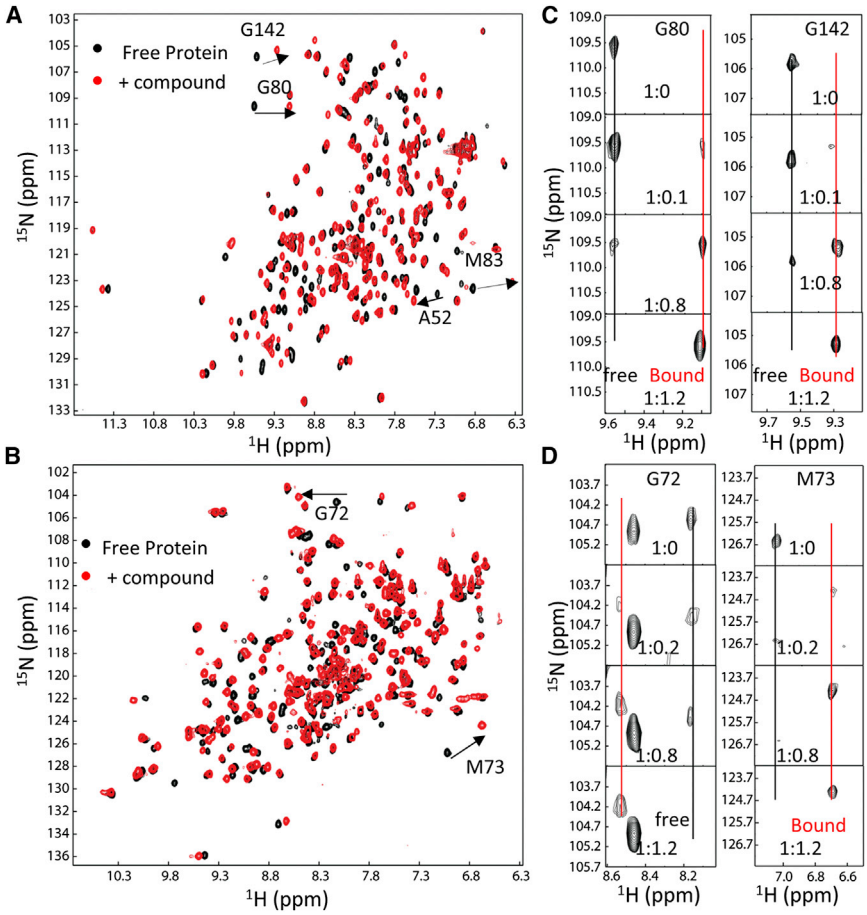

FIGURE 1 Interaction between ParEs and inhibitor 1 revealed by NMR. (*A*) ^{1}H-^{15}N-HSQC spectra of sParE in the presence and absence of inhibitor 1. (*B*) ^{1}H-^{15}N-HSQC spectra of pParE in the presence and absence of inhibitor 1. Spectra in the absence and presence of the inhibitor are shown in black and red, respectively. Some residues that showed chemical-shift changes are indicated with arrows. (*C*) Titration study for sParE and inhibitor 1. Only residues G80 and G152 are shown. (*D*) Titration study for pParE and inhibitor 1. Only results for G72 and M73 are shown. The black line indicates the free protein. Red line indicates the inhibitor 1-bound ParE. To see this figure in color, go online.

of the sParE signal in the ^{1}H-^{15}N-HSQC spectrum caused by inhibitor binding. CSPs were plotted against residue numbers (Fig. 3 *A*). It was demonstrated that residues from α2, β2, β6, the loop between β2 and α3, and α4 were important for the inhibitor interaction (Fig. 3 *A*). The most affected residues (CSP $>$ 0.3 ppm) included residues 49, 52, 55, 77, 78, 80–83, 85, 96, 141, and 174. Residues with CSPs between 0.2 and 0.3 ppm included residues 48, 51, 53, 54, 98, 122, 123, 125, 137, 138, 140, 142, 171, 170, and 173 (Fig. 3 *A*). pParE and sParE showed similar binding patterns. The amino acids in pParE that were most affected by compound binding, with CSP $>$ 0.3 ppm, included residues 38, 39, 43, 45, 67, 71–73, 86, 87, and 164. Residues with CSPs between 0.2 and 0.3 ppm included residues 42, 46, 47, 50, 75, 85, 89, and 115 (Fig. 3 *B*). It is interesting that residues from β3 of sParE, including E137, I138, R140, D141, and G142, showed clear CSP upon inhibitor binding, whereas no residue from this region of pParE showed any CSP (Fig. S6). It is possible that this difference may give rise to different binding affinities to the inhibitor.

To further understand the orientation of the inhibitor in complex with the ParEs in solution, we carried out a NOESY-TROSY experiment using a ^{15}N/^{13}C/^{2}H-labeled sample mixed with the inhibitor. Since the aliphatic and H_{α} protons of ParE are replaced with deuterium, the signals observed in the NOESY experiment will be the NOEs between amide protons from ParE and protons from the inhibitor. For sParE, NOEs between residues from α2, β2, β6, and the loop between β2 and α3 and inhibitor 1 were observed, which is in agreement with the x-ray structure of the complex (Fig. 3, *C* and *D*). For pParE, residues from the same regions showed NOEs with the inhibitor, suggesting that it binds to pParE in an orientation similar to that observed for sParE (Fig. 3 *D*).

Inhibitor 1 binds to both ParEs with different affinities

We measured the binding of inhibitor 1 against both ParEs using SPR. The SPR studies showed that inhibitor 1 has an affinity of K_D = 6.9 nM against sParE (Fig. 4 *A*) and K_D = 750 nM against pParE (Fig. 4 *B*). In an effort to understand why the inhibitor binds to sParEs with 100-fold more potency than pParE, we made mutations in α2, which is an important region for inhibitor binding. sParE has an alanine residue at position 52. In pParE, the equivalent residue is Ser-42. Both residues exhibited NOEs with the methyl group of the inhibitor (Fig. 3 *C*). It is hypothesized that

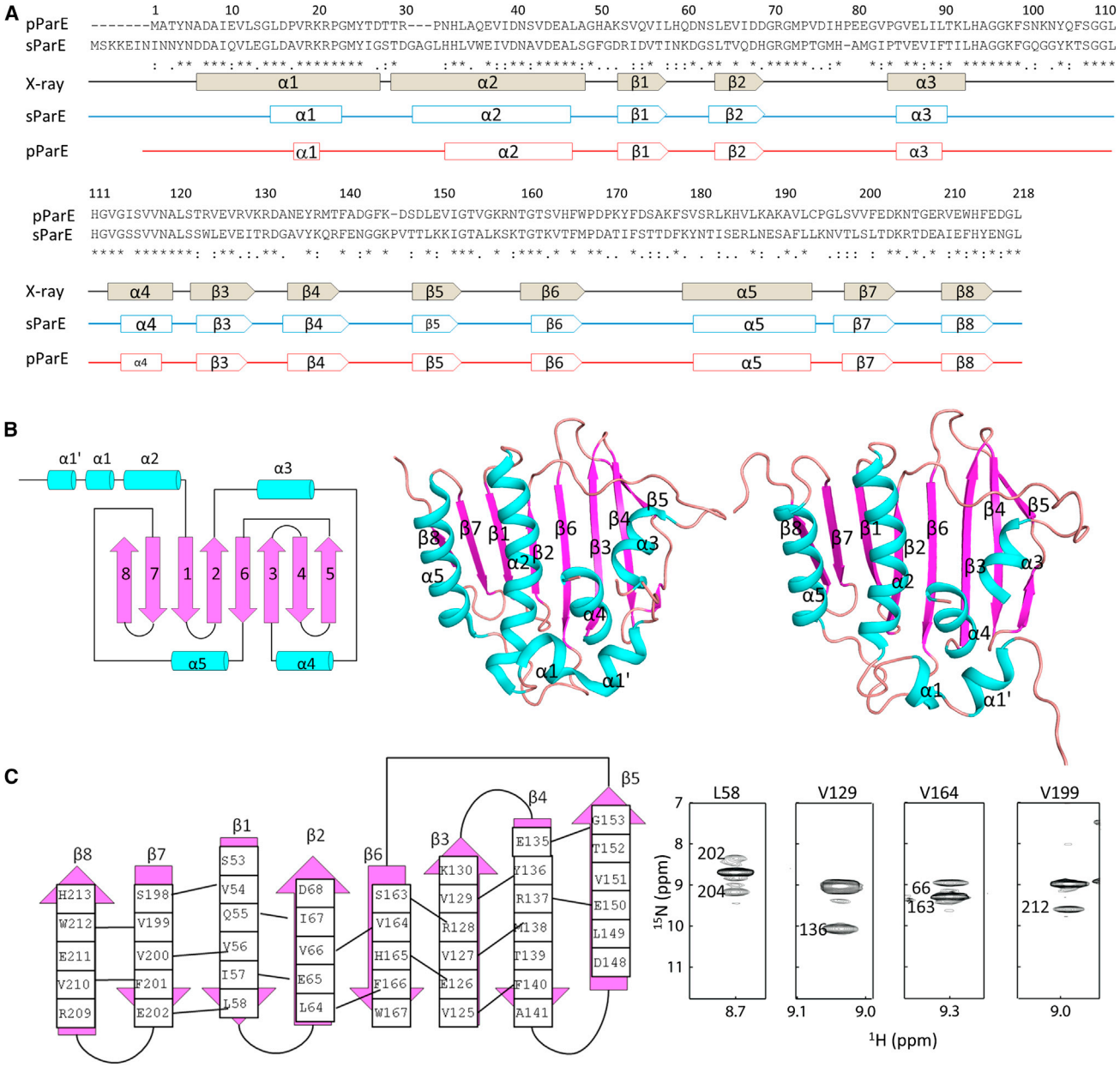

FIGURE 2 Structural analysis of pParE and sParE. (*A*) Secondary-structure analysis of ParEs in the presence of inhibitor 1. The secondary structure of the proteins was obtained based on TALOS+ prediction (27). The secondary structure derived from the x-ray structure of sParE (PDB ID: 4LP0) is shown with black lines and labeled as x-ray. The α-helix, β-strand, and loop are shown with a box, arrow, and line, respectively. The NMR structural information for sParE and pParE is indicated by blue and red lines, respectively. (*B*) Homology model of pParE. Left panel: structural topology of the ParEs' active domain. The α-helix, β-strand, and loop are shown with a box, arrow, and line, respectively. Middle panel: structure of sParE. This structure was plotted using PyMOL (http://www.pymol.org). For clarity, inhibitor 1 (PDB ID: 4LP0) is not shown. Right panel: homology model of pParE. The homology model was obtained as described in Materials and Methods. (*C*) Verification of the model by NOE experiments. Left panel: residues forming β-strand structures based on TALOS+ analysis. Lines are NOEs observed for the β-strands. Right panel: NOE observed in β-strands. Selected strip plots were obtained from a NOESY-TROSY experiment of pParE in complex with inhibitor 1. Residues having NOEs with L58, V129, V164, and V199 are labeled with the residue name and sequence number. To see this figure in color, go online.

the difference in the amino acid side chain (A versus S) is the cause of the binding discrepancy between the two enzymes. Additionally, the published x-ray crystal structure of the sParE-inhibitor complex reveals that the Cβ carbon of A52 makes close contact with the methyl group of the inhibitor, leading to a favorable hydrophobic interaction. To test this hypothesis, we made two ParE mutants. SPR studies showed that sParE A52S and pParE S42A exhibited a K_D of 32 nM and 297 nM, respectively, against the inhibitor (Fig. 4, *C* and *D*). For the pParE S42A mutation, the off-rate was reduced from 0.89 $\pm$ 0.005 to 0.15 $\pm$ 0.0037 S^{-} (Fig. 4 *E*). As expected, compared with wild-type proteins,

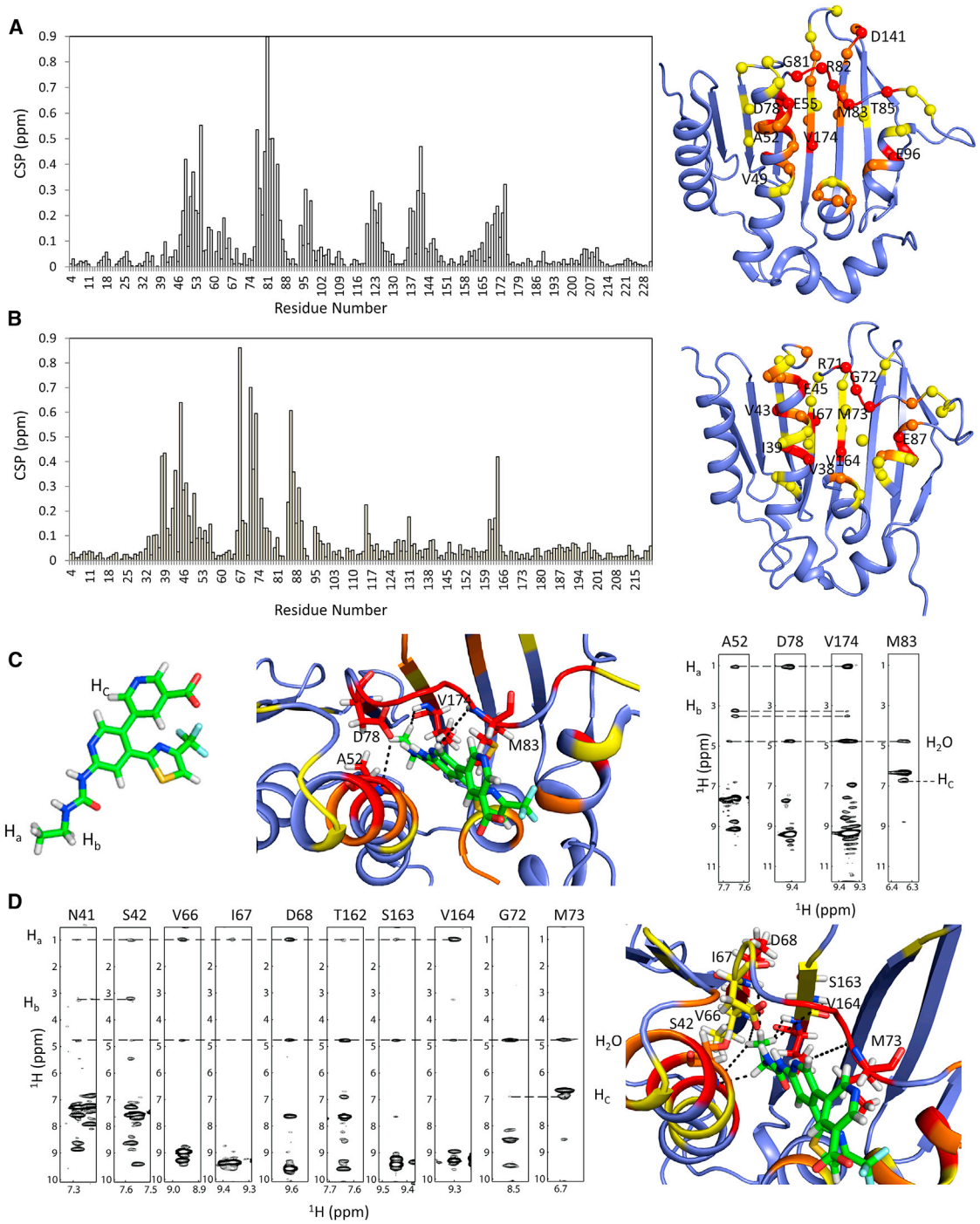

FIGURE 3 ParE-inhibitor 1 interaction. (*A*) CSP caused by inhibitor 1 binding. Left panel: CSP plotted against residue number. Right panel: residues of sParE that showed CSP in the presence of the inhibitor. The structure of sParE (PDB ID: 4LP0) is shown. For clarity, the inhibitor is not shown in the figure. (*B*) CSP of pParE induced by inhibitor 1. Left panel: CSP plotted against residue number. Right panel: residues of pParE that showed CSP in the presence of inhibitor 1. The model of pParE is shown. For clarity, the loop between α3 and α4 is not shown. (*C*) NOEs between sParE and inhibitor 1. Left panel: inhibitor 1 obtained in the crystal structure (PDB ID: 4LP0). Protons having NOEs with proteins are labeled in lowercase letters. Middle panel: crystal structure of the sParE and inhibitor 1 complex. Left panel: NOEs observed between amide protons and inhibitor protons. Right panel: strip plot of the NOESY-TROSY spectrum of sParE-inhibitor complex. (*D*) Strip plot of the NOESY-TROSY spectrum of pParE. Residues having NOEs with inhibitor 1 are shown in the left panel. Right panel: the modeled pParE-inhibitor 1 complex. The ParE-inhibitor 1 model was generated by aligning the modeled pParE structure and inhibitor 1 structure to the sParE-inhibitor 1 complex (PDB ID: 4LP0). The Cα atoms of residues with CSPs are shown with a sphere. Residues with CSPs of >0.3 ppm, 0.2–0.3 ppm, and 0.1–0.2 ppm are shown in red, brown, and yellow, respectively. To see this figure in color, go online.

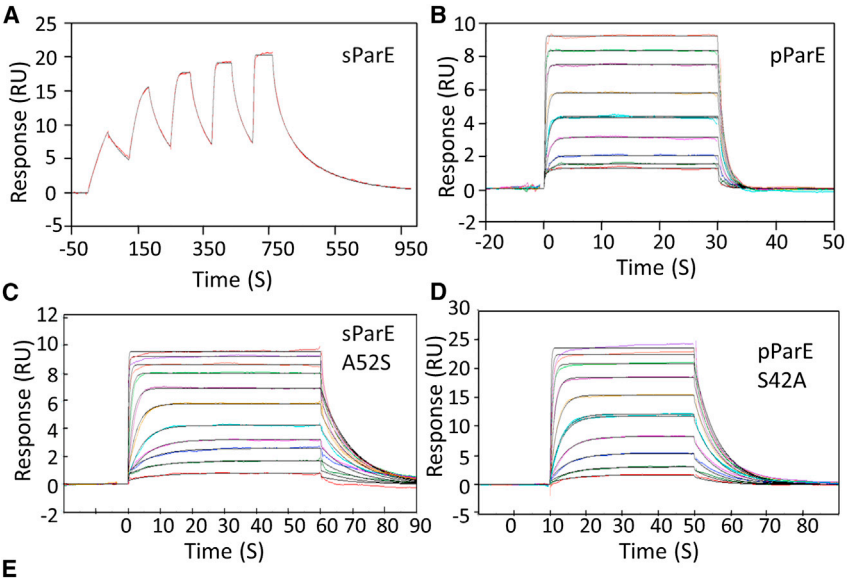

FIGURE 4 SPR results for ParE and inhibitor 1 interactions. (*A*) sParE and inhibitor 1 interaction. (*B*) pParE and inhibitor 1 interaction. (*C*) sParE A52S and inhibitor 1 interaction. (*D*) pParE S42A and inhibitor 1 interaction. (*E*) SPR and thermal stability assay of ParEs. To see this figure in color, go online.

E

	S. pn		*P. ae*	
	Wild type	A52S	Wild type	S42A
Kd (nM)	7	32	705	297
Rmax (RU)	21	7	8	21
Koff(S^{-1})	0.095	0.103	0.89	0.15
Kon($M^{-1}S^{-1}$)(×10^6)	14	3.3	1.3	0.51
Tm (°C)	47.6	44.6	43.5	48.2

mutation of sParE at position 52 to the residue in pParE reduced its binding affinity. On the other hand, mutation of pParE to the residue in the corresponding sParE showed enhanced binding affinity. NMR studies showed that the mutation did not cause conformational changes (Fig. S7). We also carried out a thermal stability assay to assess the effect of the mutation on protein stability (Figs. 4 *D* and S8). The T_m of wild-type sParE and pParE was 47.6°C and 43.5°C, respectively. Interestingly, the T_m of sParE A52S and pParE S42A was 44.6°C and 48.2°C, respectively. Protein stability may contribute to the inhibitor binding affinity or affect the off-rate. It is surprising to observe such large changes for a protein with a single mutation, suggesting that one should conduct careful structure-activity relationship studies before applying the structural data for a G^+ bacteria inhibitor to the design of a G^- bacteria inhibitor.

DISCUSSION

We prepared pParE and sParE to characterize their interactions with inhibitor 1. Since structural data for pParE have not yet been reported, we were especially interested in examining the difference between the two proteins with regard to molecular recognition. Both ParEs produced a well-dispersed ^{1}H-^{15}N-HSQC spectrum (Fig. 1) and were shown to form tight complexes with inhibitor 1 in solution (Fig. 4). A slow exchange between ParE and inhibitor 1 was observed and the complexes were stable during NMR data acquisition, which is consistent with the SPR results (Figs. 1 and 4 *E*). Additionally, the overall fold of the two proteins was very similar in solution, which is not surprising since they share high sequence homology (Fig. 3). Predictably, the NMR data confirmed binding of inhibitor 1 at the ATP pocket for both sParE and pParE (Fig. 3). Importantly, although inhibitor 1 bound to both pParE and sParE with a K_D in the nanomolar range, the binding did not cause any secondary changes on ParEs (Figs. S2–S5). To our knowledge, our results provide the first structural evidence that such inhibitors affect the chemical environment around the ATP binding site without causing any secondary structural changes on ParEs.

Our SPR study demonstrated, however, that the binding affinity of inhibitor 1 to pParE is 100-fold weaker than that to sParE (Fig. 4). This difference may arise from the difference in amino acids in the ATP binding pocket (Fig. S6). Upon inspection of the sParE-inhibitor 1 crystal structure (18), we noticed that the compound interacts with A52. The equivalent position in pParE is Ser-42. Since a previous study by Bellon et al. (30) showed that a single residue was responsible for the differential inhibition of *E. coli*

GyrB and *E. coli* ParE by novobiocin, we decided to investigate the effect of swapping these residues between sParE and pParE.

Mutation of A at position 52 of sParE to a serine residue at the equivalent position of pParE resulted in a protein (A52S) with a lower binding affinity to the inhibitor than the wild-type (Fig. 4). On the other hand, the S42A mutation of pParE showed a higher inhibitor binding affinity than the wild-type. These single mutations did not cause any structural changes as shown by NMR spectroscopy (Fig. S7). Interestingly, the T_m values of the mutant proteins were significantly different from those of their wild-type analogs (Figs. 4 and S8). CSP experiments also showed that the inhibitor bound to the ATP binding pocket. A difference was also observed for these two ParEs (Figs. 3 and S6), which may have contributed to the different K_D values. These findings also suggest that inhibitor 1 did not induce global conformation changes in ParE proteins from G^- and G^+ bacteria. Instead, differences in binding affinity were due to differences in amino acids at the active site. To overcome this challenge in developing broad-spectrum antibacterial agents, researchers need to carefully investigate protein-inhibitor interactions using different biophysical experiments. Furthermore, our results also imply that drug-discovery teams working on G^- pathogens should use proteins from the targeted bacteria for their assays, since a small structural difference can have a large impact on inhibitor potency.

In conclusion, we have reported the first (to our knowledge) structural data for the ParE protein of *P. ae* and studied its interactions with a known *bis*-pyridylurea inhibitor in solution. The results presented here, obtained from various biophysical experiments, provide a better understanding of the development of lead compounds against sParE and pParE, and will aid the discovery of more potent inhibitors for G^+ and G^- pathogens.

SUPPORTING MATERIAL

Eight figures are available at http://www.biophysj.org/biophysj/supplemental/S0006-3495(15)01001-2.

AUTHOR CONTRIBUTIONS

C.K., J.C., J.H., and T.H.K. designed the experiments. H.Q.N., Y.L.W., and M.Y.L. expressed and purified proteins. J.C., Z.Y.P., and Y.X.W. synthesized and selected the compound. C.K. and Y.L. conducted and analyzed NMR experiments. B.L. conducted and analyzed the SPR experiment. N.H.B.A. and A.W.H. conducted thermal-shift studies. C.K., Y.L., J.C., B.L., A.W.H., J.H., and T.H.K. wrote the manuscript.

ACKNOWLEDGMENTS

This work was supported by the Biomedical Research Council of A*STAR, Singapore, and by A*STAR JCO grants 1231B015 and 1331A028.

REFERENCES

1. Stein, G. E., and T. Babinchak. 2013. Tigecycline: an update. *Diagn. Microbiol. Infect. Dis.* 75:331–336.
2. Miller, J. R., and G. L. Waldrop. 2010. Discovery of novel antibacterials. *Expert Opin. Drug Discov.* 5:145–154.
3. Spellberg, B., M. Blaser, …, D. N. Gilbert; Infectious Diseases Society of America (IDSA). 2011. Combating antimicrobial resistance: policy recommendations to save lives. *Clin. Infect. Dis.* 52 (*Suppl 5*):S397–S428.
4. El-Gamal, M. I., and C. H. Oh. 2010. Current status of carbapenem antibiotics. *Curr. Top. Med. Chem.* 10:1882–1897.
5. Silver, L. L. 2011. Challenges of antibacterial discovery. *Clin. Microbiol. Rev.* 24:71–109.
6. Walsh, C. 2003. Where will new antibiotics come from? *Nat. Rev. Microbiol.* 1:65–70.
7. Bush, K., and M. J. Pucci. 2011. New antimicrobial agents on the horizon. *Biochem. Pharmacol.* 82:1528–1539.
8. Champoux, J. J. 2001. DNA topoisomerases: structure, function, and mechanism. *Annu. Rev. Biochem.* 70:369–413.
9. Škedelj, V., T. Tomašić, …, A. Zega. 2011. ATP-binding site of bacterial enzymes as a target for antibacterial drug design. *J. Med. Chem.* 54:915–929.
10. Charifson, P. S., A. L. Grillot, …, D. Stamos. 2008. Novel dual-targeting benzimidazole urea inhibitors of DNA gyrase and topoisomerase IV possessing potent antibacterial activity: intelligent design and evolution through the judicious use of structure-guided design and structure-activity relationships. *J. Med. Chem.* 51:5243–5263.
11. Crisona, N. J., T. R. Strick, …, N. R. Cozzarelli. 2000. Preferential relaxation of positively supercoiled DNA by E. coli topoisomerase IV in single-molecule and ensemble measurements. *Genes Dev.* 14:2881–2892.
12. Surivet, J. P., C. Zumbrunn, …, M. Boehme. 2013. Design, synthesis, and characterization of novel tetrahydropyran-based bacterial topoisomerase inhibitors with potent anti-gram-positive activity. *J. Med. Chem.* 56:7396–7415.
13. Tari, L. W., X. Li, …, J. Finn. 2013. Tricyclic GyrB/ParE (TriBE) inhibitors: a new class of broad-spectrum dual-targeting antibacterial agents. *PLoS One.* 8:e84409.
14. Bolon, M. K. 2009. The newer fluoroquinolones. *Infect. Dis. Clin. North Am.* 23:1027–1051.
15. Drlica, K., H. Hiasa, …, X. Zhao. 2009. Quinolones: action and resistance updated. *Curr. Top. Med. Chem.* 9:981–998.
16. Black, M. T., and K. Coleman. 2009. New inhibitors of bacterial topoisomerase GyrA/ParC subunits. *Curr. Opin. Investig. Drugs.* 10:804–810.
17. Alt, S., L. A. Mitchenall, …, L. Heide. 2011. Inhibition of DNA gyrase and DNA topoisomerase IV of Staphylococcus aureus and Escherichia coli by aminocoumarin antibiotics. *J. Antimicrob. Chemother.* 66:2061–2069.
18. Basarab, G. S., J. I. Manchester, …, A. E. Eakin. 2013. Fragment-to-hit-to-lead discovery of a novel pyridylurea scaffold of ATP competitive dual targeting type II topoisomerase inhibiting antibacterial agents. *J. Med. Chem.* 56:8712–8735.
19. Brvar, M., A. Perdih, …, T. Solmajer. 2012. Structure-based discovery of substituted 4,5′-bithiazoles as novel DNA gyrase inhibitors. *J. Med. Chem.* 55:6413–6426.
20. Brvar, M., A. Perdih, …, T. Solmajer. 2012. In silico discovery and biophysical evaluation of novel 5-(2-hydroxybenzylidene) rhodanine inhibitors of DNA gyrase B. *Bioorg. Med. Chem.* 20:2572–2580.
21. Brvar, M., A. Perdih, …, T. Solmajer. 2010. In silico discovery of 2-amino-4-(2,4-dihydroxyphenyl)thiazoles as novel inhibitors of DNA gyrase B. *Bioorg. Med. Chem. Lett.* 20:958–962.

22. Kim, Y. M., S. Gayen, …, T. H. Keller. 2013. NMR analysis of a novel enzymatically active unlinked dengue NS2B-NS3 protease complex. *J. Biol. Chem.* 288:12891–12900.

23. Pervushin, K., A. Ono, …, K. Wüthrich. 1998. NMR scalar couplings across Watson-Crick base pair hydrogen bonds in DNA observed by transverse relaxation-optimized spectroscopy. *Proc. Natl. Acad. Sci. USA.* 95:14147–14151.

24. Salzmann, M., K. Pervushin, …, K. Wüthrich. 1998. TROSY in triple-resonance experiments: new perspectives for sequential NMR assignment of large proteins. *Proc. Natl. Acad. Sci. USA.* 95:13585–13590.

25. Delaglio, F., S. Grzesiek, …, A. Bax. 1995. NMRPipe: a multidimensional spectral processing system based on UNIX pipes. *J. Biomol. NMR.* 6:277–293.

26. Johnson, B. A. 2004. Using NMRView to visualize and analyze the NMR spectra of macromolecules. *Methods Mol. Biol.* 278:313–352.

27. Shen, Y., F. Delaglio, …, A. Bax. 2009. TALOS+: a hybrid method for predicting protein backbone torsion angles from NMR chemical shifts. *J. Biomol. NMR.* 44:213–223.

28. Williamson, M. P. 2013. Using chemical shift perturbation to characterise ligand binding. *Prog. Nucl. Magn. Reson. Spectrosc.* 73:1–16.

29. Biasini, M., S. Bienert, …, T. Schwede. 2014. SWISS-MODEL: modelling protein tertiary and quaternary structure using evolutionary information. *Nucleic Acids Res.* 42:W252–258.

30. Bellon, S., J. D. Parsons, …, C. H. Gross. 2004. Crystal structures of Escherichia coli topoisomerase IV ParE subunit (24 and 43 kilodaltons): a single residue dictates differences in novobiocin potency against topoisomerase IV and DNA gyrase. *Antimicrob. Agents Chemother.* 48:1856–1864.

31. Li, Y., Y. X. Wong, …, C. Kang. 2015. NMR structural characterization of the N-terminal active domain of the gyrase B subunit from Pseudomonas aeruginosa and its complex with an inhibitor. *FEBS Lett.* 589 (19 Pt B):2683–2689.

32. Corbett, K. D., and J. M. Berger. 2003. Structure of the topoisomerase VI-B subunit: implications for type II topoisomerase mechanism and evolution. *EMBO J.* 22:151–163.

33. Lewis, R. J., O. M. Singh, …, D. B. Wigley. 1994. Crystallization of inhibitor complexes of an N-terminal 24 kDa fragment of the DNA gyrase B protein. *J. Mol. Biol.* 241:128–130.

34. Wigley, D. B., G. J. Davies, …, G. Dodson. 1991. Crystal structure of an N-terminal fragment of the DNA gyrase B protein. *Nature.* 351:624–629.